PROCEEDINGS OF SCIENCE

Investigating quarkonium production in proton-proton collisions with ALICE

Emilie Barreau[a,*] **for the ALICE Collaboration**

[a] *Subatech/IMT Atlantique,*
4 rue Alfred Kastler, Nantes, France

E-mail: emilie.barreau@subatech.in2p3.fr

Quarkonium production in high-energy proton-proton (pp) collisions provides a unique probe of both perturbative and non-perturbative aspects of quantum chromodynamics (QCD). Charmonium states, such as the J/ψ and ψ(2S), are produced through a two-stage process involving hard parton-parton scatterings followed by non-perturbative hadronization. Precise measurements are essential to constrain theoretical models and improve our understanding of these mechanisms. In this proceeding, preliminary results on the J/ψ production cross section at $\sqrt{s}$ = 13.6 TeV, measured by ALICE, will be shown. Thanks to the new Muon Forward Tracker (MFT), the separation of prompt and non-prompt J/ψ production is now possible at forward rapidity (2.5 < y < 3.6), and first measurements of their relative contributions will be presented. Additionally, the dependence of inclusive J/ψ yields on the relative charged-particle multiplicity, measured at $\sqrt{s}$ = 13 TeV in the pseudorapidity range -3.7 < η < -1.7, will be discussed. The observed steeper-than-linear trend highlights the role of multi-parton interactions. Finally, the ψ(2S)-to-J/ψ ratio and its comparison with model predictions provides further insight into the interplay between soft and hard processes in charmonium production.

The European Physical Society Conference on High Energy Physics (EPS-HEP2025)
7-11 July 2025
Marseille, France

*Speaker

ISSN 1824-8039. Published by SISSA Medialab.

PoS(EPS-HEP2025)246

1. Introduction

The strong interaction between quarks and gluons is described by the fundamental theory of quantum chromodynamics (QCD). The associated coupling constant (α_s) is small for momentum transfer larger than the QCD scale parameter $\Lambda_{\rm QCD}$ in the perturbative regime, while showing a large increase at low momentum transfer ($Q^2 \approx \Lambda_{\rm QCD}$), leading to the necessity of non-perturbative correction in this regime and the need of experimental inputs for theoretical models.

In this respect, charmonia are good probes to constrain models. As the combined charm-anticharm ($c\bar{c}$) mass is greater than $\Lambda_{\rm QCD}$, its production can be treated perturbatively. However, a non-perturbative treatment is required for the production of bound states, such as J/ψ or ψ(2S). The new measurements obtained in pp collisions at $\sqrt{s}$ = 13.6 TeV are valuable to improve models such as the Improved Color Evaporation [1] (ICEM) or Non-Relativistic QCD [2] (NRQCD) models. Moreover, in heavy-ion collisions, quarkonia are extremely sensitive to the production of quark-gluon plasma medium (QGP), a hot, deconfined state of quarks and gluons produced in these collisions. In this context, the analysis of their production would help to better understand mechanisms such as quarkonia suppression (affecting both charm and beauty) and regeneration (observed only for charm) at LHC energies. In order to properly understand those effects, the measurement in pp is essential as it provides a baseline regarding quarkonia production in heavy-ion collisions.

The ALICE [3] experiment at the LHC can measure heavy quarkonium via the leptonic decay channels: e^+e^- at midrapidity ($|\eta| < 0.9$) in the central barrel and $\mu^+\mu^-$ at forward rapidity ($-4 < |\eta| < -2.5$) with the muon spectrometer. Thanks to the Muon Forward Tracker (MFT) [4], it is now possible to separate the prompt and non-prompt J/ψ contributions using precise vertex reconstruction. Prompt J/ψ are produced at the primary vertex (PV), coming from a $c\bar{c}$ pair or radiative decay product (χ_c) and are therefore probes for the charm production, while non-prompt J/ψ are decay products of b hadrons, displaced from the PV with respect to the b hadron time of flight, providing information on beauty production.

Another new feature of Run 3 is the continuous readout system, specifically designed to support the higher interaction rates provided by the LHC. Software triggers which select collisions of interest have been designed and implemented to reduce the data size.

2. Results

2.1 J/ψ cross-section measurement at midrapidity

The J/ψ production cross section measured by ALICE in pp collisions at $\sqrt{s}$ = 13.6 TeV in the electron decay channel is presented in Fig.1 (left). The results are compared with theoretical models such as the Improved Color Evaporation Model [1] (pink), the Non-Relativistic QCD [2] (black and green), the Color Glass Condensate [5] (brown) model, and the FONLL calculations [6] (light green, only for non-prompt J/ψ). It can be observed that ICEM, CGC and NRQCD models are compatible with the data for all $p_{\rm T}$, suggesting that the main contribution comes from the prompt J/ψ at low $p_{\rm T}$ while the non-prompt J/ψ contribution is being more significant at higher $p_{\rm T}$. The Fig.1 (right) illustrates the consistency and the complementarity in $p_{\rm T}$ coverage of the ALICE [7] data from Run 2 and Run 3 with the ATLAS [8] data from Run 2.

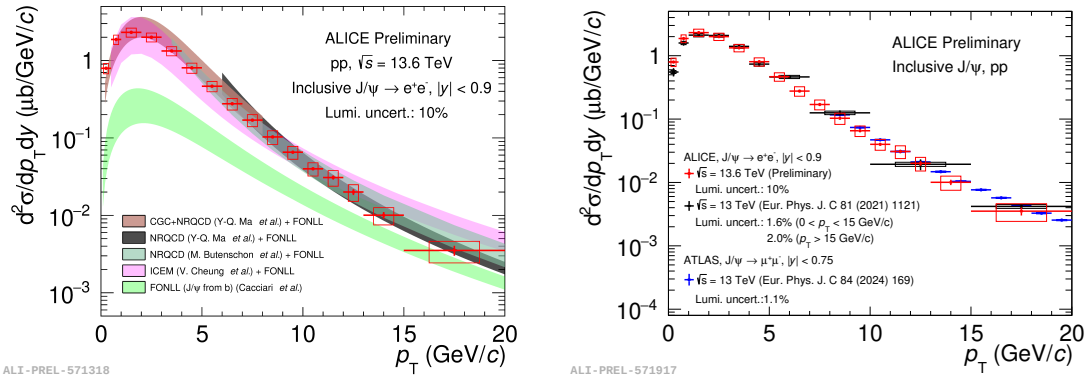

Figure 1: Left : J/ψ inclusive cross section for pp Run 3 data as a function of p_{T} and comparison with models - Right : J/ψ inclusive cross section at midrapidity from ALICE Run 2 (black) and Run 3 (red) data with ATLAS Run 2 results (blue).

2.2 Dependence of inclusive J/ψ yield on multiplicity during Run 2

The dependence of the J/ψ yield on charged-particle multiplicity provides information on high density effects such as string reconnection or collectivity, or effects of the initial state [9]. In a basic multi-parton interaction (MPI) scenario, the relationship between the J/ψ production yield $N_{\mathrm{J}/\psi}$ and multiplicity N_{ch} is expected to follow a linear trend, which differs from the data plotted in Fig.2 (left). One can see two different trends : steeper-than-linear (red, yellow and gray points) and close-to-linear (blue and green points).

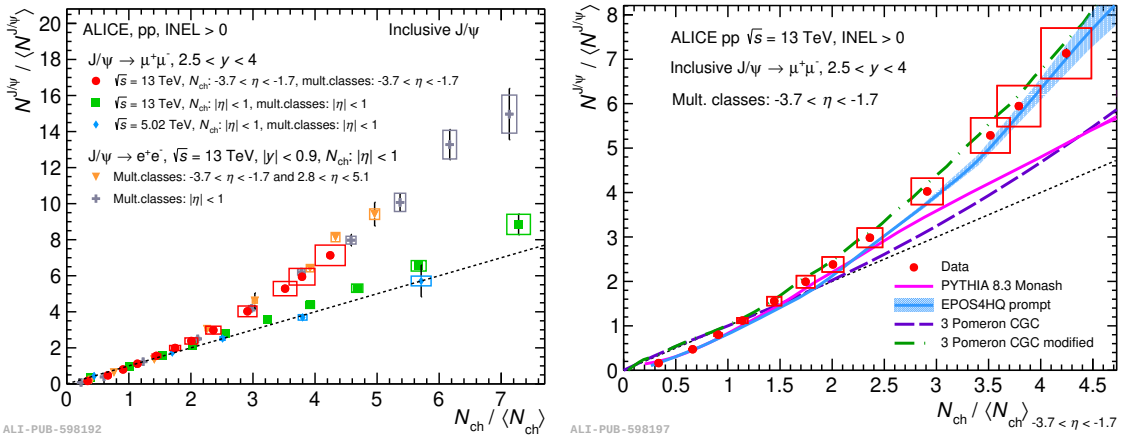

Figure 2: Left : Relative inclusive J/ψ yield as a function of relative charged-particle multiplicity N_{ch} at mid (yellow and gray points) and forward rapidity (red, blue and green points) - Right : Relative inclusive J/ψ yield as a function of relative charged-particle multiplicity N_{ch} at forward rapidity and comparison with models.

The steeper-than-linear trend is obtained by measuring the J/ψ production and the multiplicity estimator in the same pseudo-rapidity range, suggesting an autocorrelation mechanism: the choice of the pseudo-rapidity range could bias the measurement. Another explanation for this behavior would be the color reconnection included in PYTHIA[10] simulations. However, the Fig.2 (right),

comparing data at 13 TeV with models, shows that the color reconnection mechanism alone cannot reproduce the data at higher multiplicity. On the other hand, EPOS4HQ [11] and the 3 Pomeron CGC modified [12, 13] models are consistent with the measurement while including the non linear effects as well as the gluonic saturation. This may also suggests an autocorrelation mechanism. To complete the picture, the measurement of the J/ψ production at midrapidity with the multiplicity estimator at forward rapidity, with a close-to-linear trend expectation, would be beneficial to disentangle autocorrelation effects from high-density effects.

2.3 ψ(2S)-to-J/ψ ratio at mid and forward rapidity

The ψ(2S)-to-J/ψ ratio as a function of p_{T} measured at mid (left panel) and forward (right panel) rapidity is presented in Fig.3. In both rapidity ranges, the CGC + NRQCD and ICEM models are in good agreement with the data, while NRQCD overestimates the ratio at high p_{T}. This can be explained by NRQCD not giving a complete description of the production process on its own. As the ψ(2S) is a heavier and weaker bound state than the J/ψ, the ratio is expected to be smaller than one. A hint of a dependence on p_{T} is also seen, although the current experimental uncertainties don't allow for a firm conclusion.

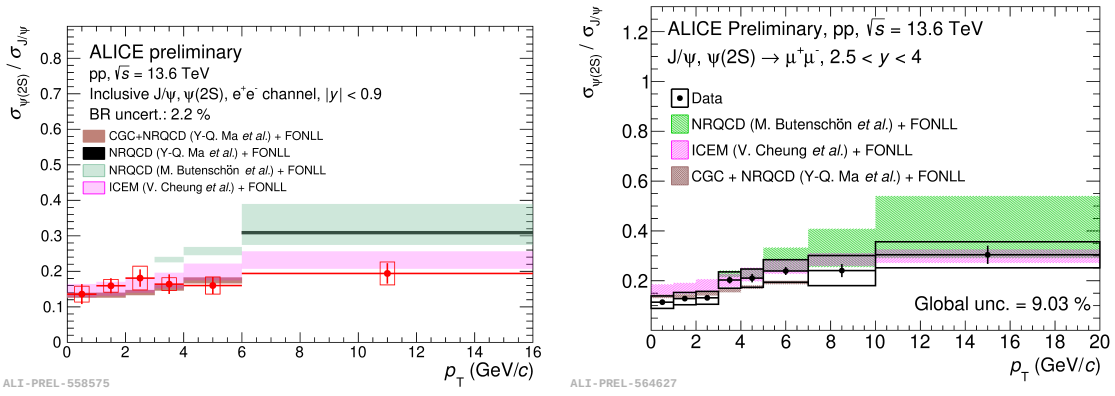

Figure 3: ψ(2S)-to-J/ψ ratio as a function of p_{T} and comparison to models at mid (left) and forward (right) rapidity.

The energy dependence of the ratio was also studied and is presented in Fig.4 (left). The ALICE results from Run 2 (13 TeV) and Run 3 (13.6 TeV) are compared with the measurement from several experiments, including LHCb [14], PHENIX [15], E705 [16] and ISR [17], at different center-of-mass energies. Within the uncertainties, the ψ(2S)-to-J/ψ ratio shows a constant value and therefore no energy dependence. In Fig.4 (right), the ALICE data from Run 2 (blue) and Run 3 at mid and forward rapidity (red and black) are presented. The results are consistent in both rapidity ranges and the Run 2/Run 3 data are compatible within the 3σ confidence level.

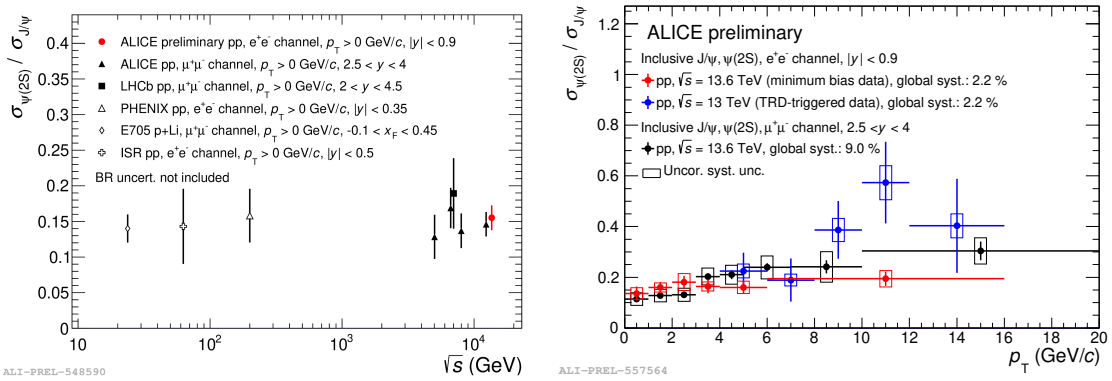

Figure 4: Left : ψ(2S)-to-J/ψ ratio as a function of center-of-mass energy - Right : ψ(2S)-to-J/ψ ratio as a function of p_{T} at mid and forward rapidity in Run 3 (respectively red and black points) and Run 2 data at midrapidity (blue points).

2.4 Prompt/non-prompt J/ψ separation at mid and forward rapidity

The separation of prompt and non-prompt J/ψ is valuable to strengthen our knowledge on quarkonium production and to improve the current theoretical models. Thus, prompt and non-prompt contributions can be discriminated using a Lorentz-invariant observable depending on the vertex position called the pseudo-proper decay time τ (its component along the beam axis z) defined as :

$$c\tau_{\mathrm{z}} = c\frac{|z_{\mathrm{J}/\psi} - z_{\mathrm{vtx}}|M_{\mathrm{J}/\psi}}{p_{\mathrm{z}}} \tag{1}$$

It depends on the decay vertex position of the J/ψ ($z_{\mathrm{J}/\psi}$), the primary vertex/interaction point position (z_{vtx}), invariant mass $M_{\mathrm{J}/\psi}$ and the longitudinal momentum p_{z}. As the relativistic longitudinal boost increases the time of flight of b hadrons, the τ_{z} value for non-prompt contribution tends to be above zero, unlike the prompt contribution.

The amount of non-prompt J/ψ with respect to the prompt J/ψ can be expressed as :

$$f'_{\mathrm{B}} = \frac{N_{\mathrm{J}/\psi\leftarrow\mathrm{h_B}}}{N_{\mathrm{J}/\psi\leftarrow\mathrm{h_B}} + N_{\mathrm{J}/\psi}}, \qquad f_{\mathrm{B}} = \left(1 + \frac{1 - f'_{\mathrm{B}}}{f'_{\mathrm{B}}}\frac{\langle A\cdot\epsilon\rangle_{\mathrm{non-prompt}}}{\langle A\cdot\epsilon\rangle_{\mathrm{prompt}}}\right)^{-1}, \tag{2}$$

with f'_{B} being the uncorrected non-prompt fraction and f_B the corrected one including the acceptance-efficiency correction.

Fig.5 (left) shows the non-prompt J/ψ fraction at forward rapidity increasing with p_{T}. The results are compatible with LHCb [18] in the same η range down to 0 GeV/c. These results are also compared to the measurements from ALICE and ATLAS [19] at mid-rapidity in Fig.5 (right). In agreement with the B production kinematics, f_{B} appears to be higher at midrapidity for both ALICE and ATLAS data. This figure emphasizes the complementarity of the different experiments to provide data over a large p_{T} range. Thanks to the MFT, this measurement of the non-prompt fraction at forward rapidity is now possible with ALICE.

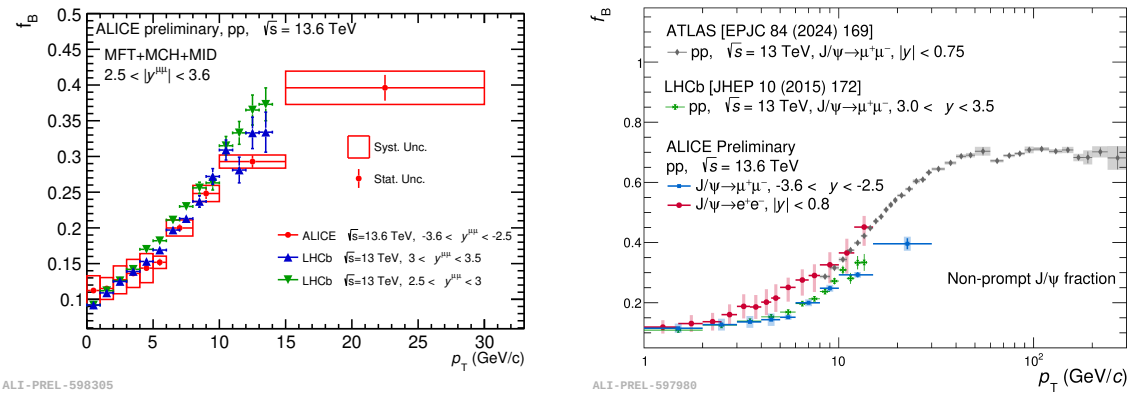

Figure 5: Left : J/ψ non-prompt fraction as a function of p_{T} at forward rapidity compared to LHCb results Right : J/ψ non-prompt fraction as a function of p_{T} from ALICE at mid and forward rapidity (respectively blue and red points) with LHCb and ATLAS results (respectively green and gray points).

3. Conclusion

The study of quarkonium production in proton-proton collisions provides valuable information about the production mechanisms, including the role of MPIs and initial parton density. The new measurements obtained in Run 3 will help to constrain the theoretical models and will also be a baseline for heavy-ion studies, especially regarding the studies on suppression and recombination effects in the QGP.

References

[1] Cheung et al. Phys. Rev. D 98 (2018).

[2] K. Zalewski, Acta Phys. Polon. B 29 (1998).

[3] ALICE Collaboration, JINST 19 (2024) P05062.

[4] ALICE Collaboration, CERN-LHCC-2015-001 (2015).

[5] Ma et al. Phys. Rev. Lett. 113 (2014).

[6] Cacciari et al. JHEP 10 137 (2012).

[7] ALICE Collaboration, Eur. Phys. J. C 81 (2021).

[8] ATLAS Collaboration, Eur. Phys. J. C 84 (2024).

[9] ALICE Collaboration, CERN-EP-2025-070 (2025).

[10] C. Bierlich et al, SciPost Phys. Codeb (2022) 8.

[11] J. Zhao, J. Aichelin, P.B. Gossiaux and K. Werner, Phys. Rev. D 109 (2024) 054011.

[12] E. Levin, I. Schmidt and M. Siddikov, Eur. Phys. J. C 80 (2020) 560.

[13] E. Gotsman and E. Levin, Eur. Phys. J. C 81 (2021) 99.

[14] LHCb Collaboration, J. High Energ. Phys. 243 (2024).

[15] PHENIX Collaboration, Phys. Rev. C 205 (2022) 064912.

[16] E705 Collaboration, Phys. Rev. Lett. 70 (1993) 383.

[17] ISR Collaboration, Nucl. Phys. B 142 (1978) 29.

[18] LHCb Collaboration, J. High Energ. Phys. 172 (2015).

[19] ATLAS Collaboration, Eur. Phys. J. 84 (2024) 169.